




ORIGINAL RESEARCH

Prediction Model for Contractile Function of Circulatory Death Donor Hearts Based on Microvascular Flow Shifts During Ex Situ Hypothermic Cardioplegic Machine Perfusion

Lars Saemann , MSc, ECCP; Matthias Kohl , PhD; Gábor Veres, MD, PhD; Sevil Korkmaz-Icöz, PhD; Anne Großkopf, PhD; Matthias Karck, MD, PhD; Andreas Simm , PhD; Folker Wenzel, MD, PhD; Gábor Szabó, MD, PhD

BACKGROUND: Hearts procured from circulatory death donors (DCD) are predominantly maintained by machine perfusion (MP) with normothermic donor blood. Currently, DCD heart function is evaluated by lactate and visual inspection. We have shown that MP with the cardioplegic, crystalloid Custodiol-N solution is superior to blood perfusion to maintain porcine DCD hearts. However, no method has been developed yet to predict the contractility of DCD hearts after cardioplegic MP. We hypothesize that the shift of microvascular flow during continuous MP with a cardioplegic preservation solution predicts the contractility of DCD hearts.

METHODS AND RESULTS: In a pig model, DCD hearts were harvested and maintained by MP with hypothermic, oxygenated Custodiol-N for 4 hours while myocardial microvascular flow was measured by Laser Doppler Flow (LDF) technology. Subsequently, hearts were perfused with blood for 2 hours, and left ventricular contractility was measured after 30 and 120 minutes. Various novel parameters which represent the LDF shift were computed. We used 2 combined LDF shift parameters to identify bivariate prediction models. Using the new prediction models based on LDF shifts, highest r^2 for end-systolic pressure was 0.77 ($P=0.027$), for maximal slope of pressure increment was 0.73 ($P=0.037$), and for maximal slope of pressure decrement was 0.75 ($P=0.032$) after 30 minutes of reperfusion. After 120 minutes of reperfusion, highest r^2 for end-systolic pressure was 0.81 ($P=0.016$), for maximal slope of pressure increment was 0.90 ($P=0.004$), and for maximal slope of pressure decrement was 0.58 ($P=0.115$). Identical prediction models were identified for maximal slope of pressure increment and for maximal slope of pressure decrement at both time points. Lactate remained constant and therefore was unsuitable for prediction.

CONCLUSIONS: Contractility of DCD hearts after continuous MP with a cardioplegic preservation solution can be predicted by the shift of LDF during MP.

Key Words: coronary microvasculature ■ Custodiol-N ■ donation after circulatory death ■ heart transplantation ■ machine perfusion ■ myocardial microcirculation ■ prediction model

Correspondence to: Lars Saemann, MSc, ECCP, Department of Cardiac Surgery, University Hospital Halle, Ernst-Grube-Straße 40, 06120 Halle (Saale), Germany. Email: lars.saemann@uk-halle.de; lars.saemann@gmx.de

These results were presented at the American Heart Association's Scientific Sessions, November 13–15, 2021. The respective meeting abstract was awarded the Paul Dudley White International Scholar Award as the highest-ranked abstract from Germany.

Supplemental Material is available at <https://www.ahajournals.org/doi/suppl/10.1161/JAHA.122.027146>

For Sources of Funding and Disclosures, see page 9.

© 2022 The Authors. Published on behalf of the American Heart Association, Inc., by Wiley. This is an open access article under the terms of the [Creative Commons Attribution-NonCommercial-NoDerivs](https://creativecommons.org/licenses/by-nc-nd/4.0/) License, which permits use and distribution in any medium, provided the original work is properly cited, the use is non-commercial and no modifications or adaptations are made.

JAHA is available at: www.ahajournals.org/journal/jaha

Nonstandard Abbreviations and Acronyms

DCD	donation after circulatory-determined death
dp/dt_{max}	maximal slope of pressure increment
dp/dt_{min}	maximal slope of pressure decrement
LDP	laser Doppler perfusion
MP	machine perfusion
PCM	pressure-contractility-matching

Organ shortage is a major limiting factor for heart transplantation. To increase the number of donor hearts, multiple centers worldwide have successfully established heart transplantation from donation after circulatory-determined death (DCD).^{1–4} DCD hearts are exposed to warm ischemia.⁵ Therefore, most clinical protocols intend to perform a functional evaluation of the DCD heart.⁵ Three retrieval protocols allow functional evaluation: (1) direct procurement of the DCD heart followed by normothermic machine perfusion (MP), (2) normothermic regional perfusion followed by normothermic MP, and (3) normothermic regional perfusion followed by static cold storage.⁵ In direct procurement, the DCD heart is harvested, and functional evaluation is performed based on visual inspection and metabolic surrogates, like lactate, during normothermic MP.⁶ During normothermic regional perfusion, the donor, including the heart, is reperfused by central extracorporeal membrane oxygenation, excluding cerebral circulation, allowing functional evaluation of the heart in situ.⁷ In the case of normothermic regional perfusion followed by normothermic MP, a second or ongoing functional evaluation in the MP system is possible.

The DCD heart is perfused with oxygenated blood collected from the organ donor during normothermic MP. Despite the remarkable success of normothermic blood perfusion in the clinical setting, we have recently shown in a porcine model of DCD that MP with hypothermic, oxygenated, crystalloid Custodiol-N preservation solution is superior to blood perfusion to recondition contractile function.⁸ Based on these preclinical results, a translation of crystalloid MP with Custodiol-N into clinical practice could be promising. Nevertheless, hypothermic MP with a cardioplegic preservation solution facilitates nonbeating transportation. Consequently, functional evaluation during MP would be impossible, inhibiting the option for the most common retrieval protocol for DCD hearts, which is direct procurement followed by MP.² Hearts procured from brain dead donors are commonly preserved by static cold storage and then transplanted without prior functional evaluation. Thus, not performing functional evaluation of the donor heart after hypothermic MP would not be critical in donation after brain death. Unlike

donation after brain death, functional or metabolic evaluation of the cardiac allograft before transplantation is essential in DCD. Functional assessment of the heart after hypothermic MP would require reperfusion with warm blood in the perfusion system. After functional evaluation, a cardioplegic arrest would have to be induced to demount the heart from the perfusion system. Both procedural steps would create additional ischemia/reperfusion periods that could harm the heart. Consequently, blood reperfusion after hypothermic crystalloid perfusion does not facilitate a realistic option to determine the contractile function of the DCD heart at the end of transportation.

Therefore, we developed a prediction model for the contractile function of the DCD heart after hypothermic, cardioplegic MP. Based on changes of myocardial microcirculation during normothermic MP, the new prediction model is based on microvascular flow shifts during hypothermic MP.⁹

METHODS

The data that support the findings of this study are available upon reasonable request.

Animals and Anesthesia

The investigations were reviewed and approved (35–9185.81/G-150/19) by the appropriate institutional Ethical Committee for Animal Experimentation. The animals received humane care.¹⁰ We sedated healthy pigs (N=8) with 40 to 50 kg of body weight by intramuscular injection of ketamine (22.5 mg/kg; Bremer Pharma, Warburg, Germany) and midazolam (0.375 mg/kg; Hameln pharma plus, Hameln, Germany). We maintained anesthesia intravenously with pentobarbital-sodium (15 mg/kg per hour; Boehringer Ingelheim Vetmedica, Ingelheim, Germany) through the ear vein. The analgesic drug Dipidolor (1.125 mg/kg per hour; Piramal Critical Care, Voorschoten, Netherlands) was given. We adjusted ventilation to maintain partial pressure of oxygen of around 200 mmHg and partial pressure of carbon dioxide of 35 to 45 mmHg. We achieved arterial and venous vascular access in the femoral artery and vein for monitoring arterial blood pressure and blood sampling.

DCD Model and MP

We opened the chest by median sternotomy and exposed the heart by pericardiotomy. We injected heparin (LEO Pharma, Neuisenburg, Germany) intravenously to achieve systemic anticoagulation. According to a previously published model, we induced circulatory death by the termination of mechanical ventilation.⁹ Within the subsequent period of 30 minutes, blood was collected in blood collection bags and the heart was harvested. After a total warm ischemic period of 30 minutes, the DCD hearts were flushed with 2 L of cold (4°C) traditional

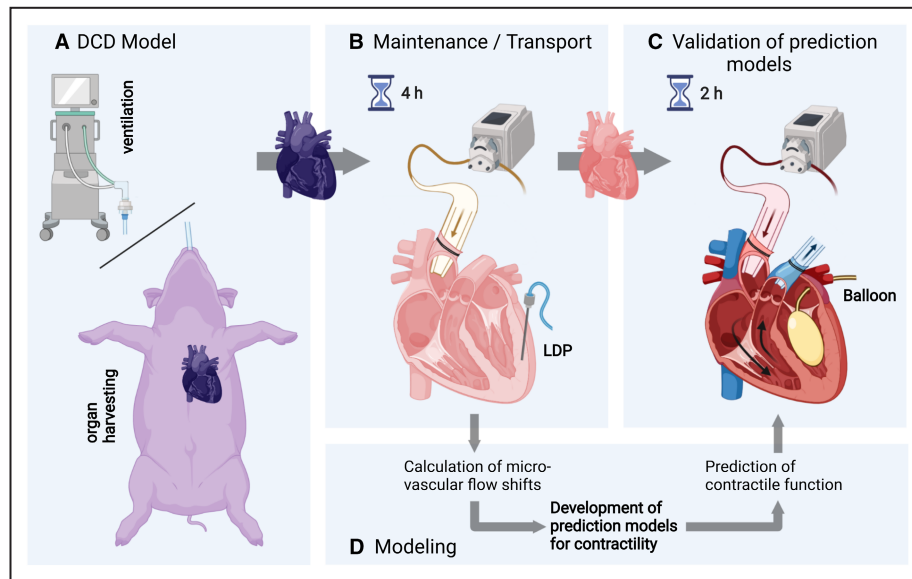


Figure 1. Donation after circulatory death model and functional analysis.

A, DCD induction by the termination of mechanical ventilation. **B**, Continuous measurement of microvascular flow by laser Doppler perfusion probe during 4 hours of hypothermic, oxygenated cardioplegic perfusion with Custodiol-N. **C**, Contractile assessment. **D**, Development of prediction models. DCD indicates donation after circulatory death; and LDP, laser Doppler perfusion. The figure was created with BioRender.

Custodiol preservation solution (Köhler Chemie GmbH, Bensheim, Germany) followed by mounting on the perfusion system (Figure 1). Then the hearts were perfused for 4 hours through the ascending aorta.

The perfusion system was primed with 2L of the novel crystalloid, cardioplegic Custodiol-N preservation solution. Characteristics of Custodiol-N are described elsewhere.⁸ The perfusion pressure was set at 20 mmHg. We continuously oxygenated the perfusate solution with an integrated oxygenator. We also measured the lactate concentration every 30 minutes (RAPID Point 500, Siemens) according to the standardized perfusion monitoring known from blood perfusion.

Reperfusion and Validation of Prediction Models

After 4 hours of maintenance perfusion, the DCD hearts were reperfused with normothermic blood for 2 hours to mimic transplantation. We adjusted a partial pressure of oxygen of 180 to 200 mmHg, partial pressure of carbon dioxide of 35 to 45 mmHg, and pH of 7.35 to 7.45. We set the perfusion pressure on 50 to 60 mmHg. To validate the prediction models for contractility, the contractile function was assessed by a left ventricular balloon catheter, inserted through the mitral valve to be filled with artificial preload volumes of 5 to 20 mL. We determined end-systolic pressure, maximal slope of pressure increment (dp/dt_{max}), and maximal slope of pressure decrement (dp/dt_{min}). Contractility was measured after 30 and 120 minutes of reperfusion. Additionally,

pressure-contractility-matching (PCM) was determined by keeping the left ventricular filling constant at 10 mL and adjusting the perfusion pressure from 20 to 100 mmHg.

Monitoring of Microvascular Flow

We continuously monitored myocardial microvascular flow during 4 hours of MP by laser Doppler perfusion (LDP) monitoring using an LDP needle probe (Perimed, Järfälla Stockholm, Sweden), inserted into the anterior wall of the left ventricle. Various novel parameters were calculated that reflect the shift of microvascular flow during hypothermic, cardioplegic MP based on our already published equations shown in Table S1.⁹ In brief, the LDP signal needs to be analyzed in periods to incorporate periodic variations no matter the LDP at a particular time point or over a time frame is of interest (Figure 2A).¹¹ We either expressed LDP as a “singular” measurement (mean over 20 seconds) periodically every 30 minutes or as an “interval” measurement (mean over 30 minutes). Additionally, the same analysis was performed with the area under the curve (AUC). We calculated the shift of relative LDP or AUC of the first interval (first 30 minutes of MP: 0 to 30 minutes), the second interval (30 to 60 minutes of MP), and the second last interval (180 to 210 minutes of MP) to the last interval (final 30 minutes: 210 to 240 minutes of MP) (Figure 2B). We also calculated the shift of relative LDP or AUC of the 20-second period at 30, 60, and 210 minutes of MP to the last 20 seconds at minute 240. We also calculated the mean shift of every interval (30 minutes) to the subsequent one over the whole course of MP.

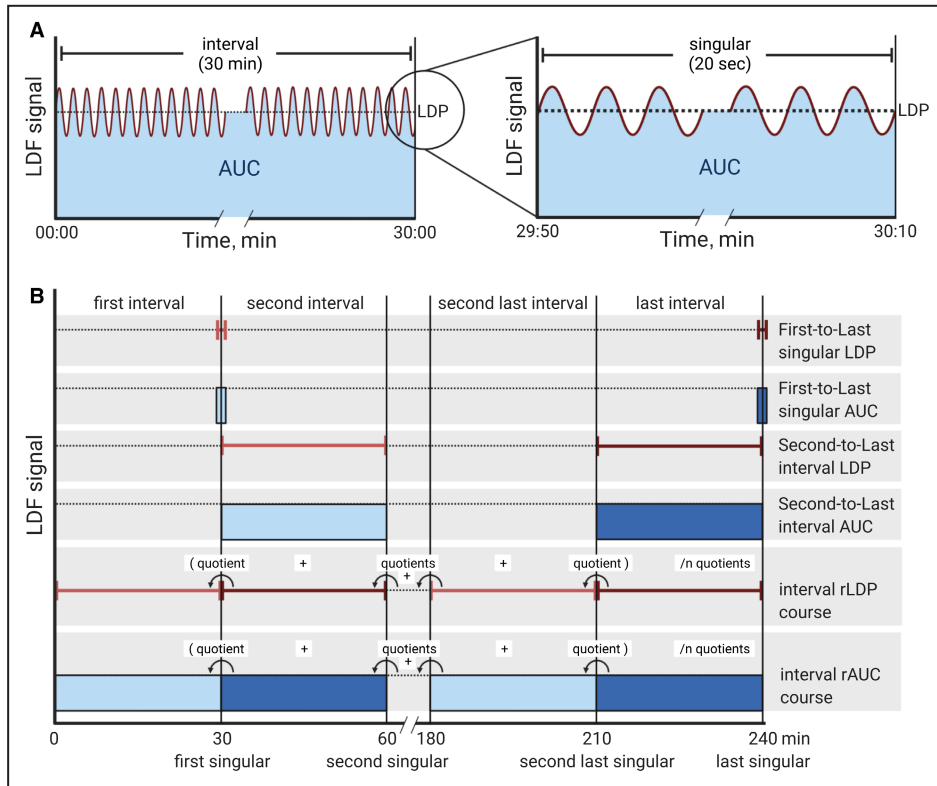


Figure 2. Models.

AUC indicates area under the curve; LDF, Laser Doppler Flow; LDP, laser Doppler perfusion; rAUC, relative AUC; and rLDF, relative LDF and shows the mean of the LDF signal over the observed period.

Workflow of Model Identification

The workflow of model identification is visualized in Figure 3 and consisted of the following steps.

Model Development

1. Development of prediction models based on 1 parameter, which reflects an individual type of microvascular flow shift during MP.

2. Development of prediction models based on 2 combined parameters that reflect different microvascular shifts during MP. With this, we calculated all possible combinations of microvascular flow shift parameters. The use of 2 combined parameters is based on the findings from a previous study, which showed that the combination of 2 parameters could incorporate more predictive power.⁹

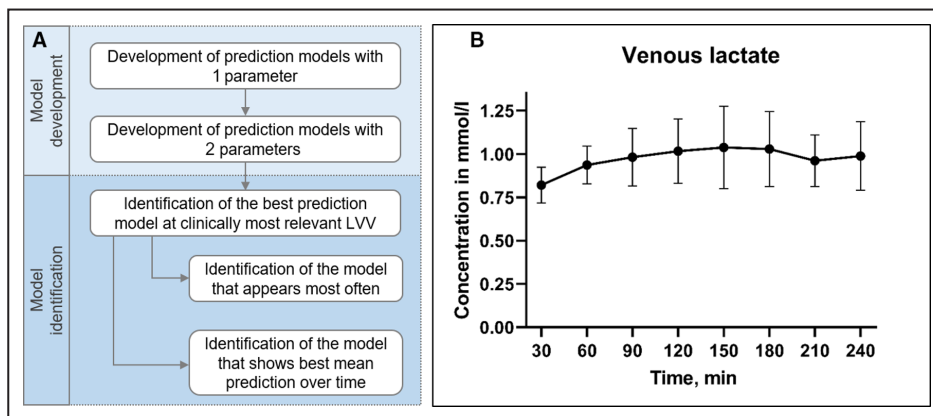


Figure 3. Workflow.

A, Model prediction and model identification. **B**, Venous lactate concentration. LVV indicates Left ventricular volume.

Model Identification

From all developed models, we identified the best model with the highest clinical relevance, based on the following criteria:

1. Predictive properties were determined based on the highest r^2 of the respective model.
2. The prediction of contractile function at an LVV of 20mL among all tested filling volumes of the left ventricle and PCM at 100mmHg among all tested perfusion pressures is most important.
3. The model, which can predict most of the contractile parameters and shows the best mean prediction over the observed reperfusion period, is defined as the best prediction model.

Statistical Analysis

Statistical analysis was performed using R and IBM SPSS Statistics for Windows (Version 20.0, IBM Corp., NY, USA). We used Pearson correlation and linear regression analysis to assess the association between contractile parameters and single covariates or 2 covariates. An F -Test was used to test the significance of models. A value of $P < 0.05$ was considered statistically significant.

RESULTS

Prediction Models With 1 Parameter

The lactate concentration remained between 0.82 and 0.98 mmol/L through 4 hours of cardioplegic perfusion

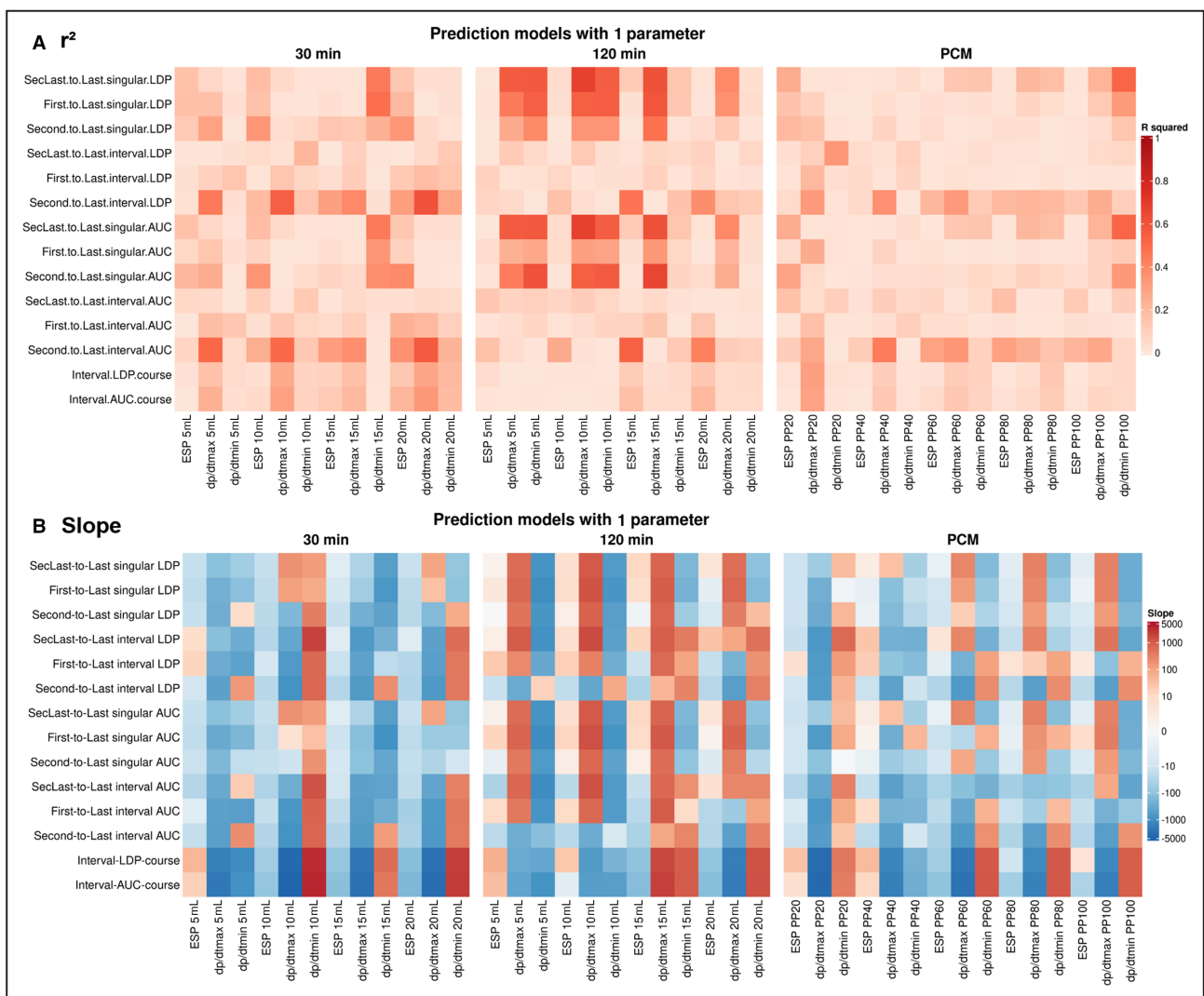


Figure 4. Heat map of prediction models with 1 parameter.

The heat map depicts the color-coded r^2 (A) or slope (B) of each prediction model shown on the left for each contractile parameter shown below at 30 and 120 minutes of reperfusion and for pressure-contraction-matching. N=8. AUC indicates area under the curve; dp/dt_{max}, Maximal pressure increase; dp/dt_{min}, Maximal pressure decrease; ESP, end-systolic pressure; LDP, laser Doppler perfusion; PCM, pressure-contraction-matching; PP, perfusion pressure; and SecLast, second-last.

and was unsuitable for prediction because it did not show relevant variation (Figure 2). Prediction models based on 1 parameter showed a predominantly heterogeneous heat map formation (Figure 4) when predicting contractile function after 30 minutes of reperfusion. Regarding the prediction at 120 minutes of reperfusion, a cluster building is visible for different dp/dt_{max} and dp/dt_{min} at different LVVs with a significant r^2 (Figure 5) in the models second last to last singular LDP, first to last singular LDP, second last to last singular AUC, and second to last singular AUC. Only 2 models with significant r^2 could be developed for PCM, both for dp/dt_{min} at 100mmHg of perfusion pressure.

Prediction Models With 2 Parameters

Contrary to prediction models with 1 parameter, prediction models based on 2 combined parameters (Figure 6) showed separated multiple cluster building with high r^2 values at various LVVs at 30, 120 minutes, and PCM. According to the algorithm shown above, the best models per contractile parameter, considering clinically relevant criteria like LVV and PP over all time points and PCM, are shown in Figure 7. Second to last singular LDP shift was part of most 2-variable prediction models. First to last singular LDP shift was the second most often part of 2-variable prediction models. The combination of both was the prediction

model, which occurred most frequently. Second to last singular or interval AUC was the third most often 1 of 2 variables, which built a prediction model. Considering PCM and mean prediction over time, we could predict end-systolic pressure best by combining interval-LDP-course and interval-AUC-course. For all performance parameters, end-systolic pressure, dp/dt_{max} , and dp/dt_{min} , predictability was highly similar at 30 minutes of reperfusion. At 120 minutes of reperfusion, the predictability of dp/dt_{max} was improved but decreased for PCM. For dp/dt_{min} we detected the opposite.

DISCUSSION

The finding that prediction models based on 2 combined parameters and results from our previous study on normothermic blood perfusion in a porcine DCD model.⁸ Therefore, this study confirms that in hypothermic, cardioplegic MP, 2 combined variables provide more predictive information about contractile function during reperfusion than 1 parameter.

In contrast to our results from normothermic blood perfusion, the 2 most frequently incorporated LDP shift parameters are not "interval"-based but of "singular" measurement character. Presumably, during

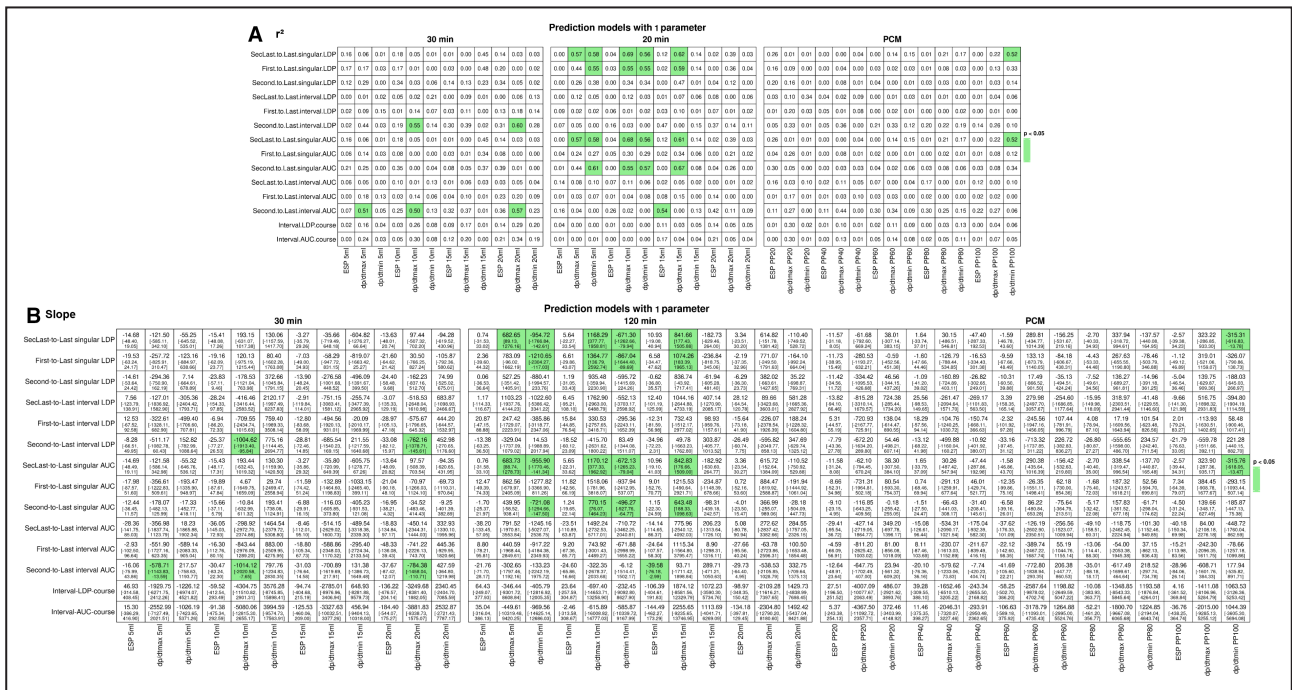


Figure 5. r^2 values for prediction models with 1 parameter.

The heat map depicts the actual r^2 values (A) or slope (B) of each prediction model shown on the left for each contractile parameter shown below at 30 and 120 minutes of reperfusion and for pressure-contractility-matching. Significant ($P < 0.05$) r^2 are marked green. N=8. AUC indicates area under the curve. dp/dt_{max} , Maximal pressure increase, dp/dt_{min} , Maximal pressure decrease; ESP, end-systolic pressure; LDP, later Doppler decrease; PCM, pressure-contractility-matching; PP, perfusion pressure; and SecLast, second last.

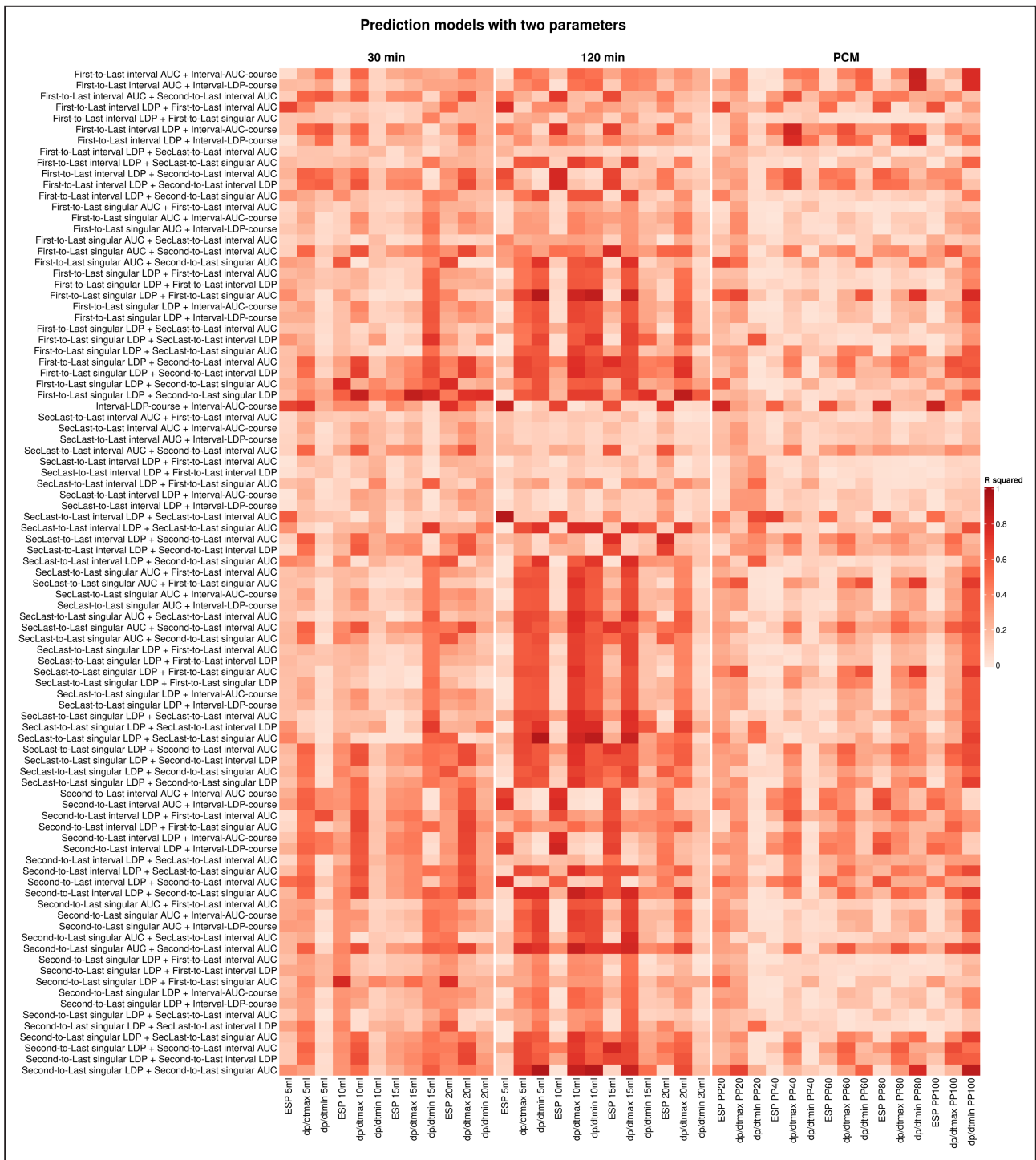


Figure 6. Heat map of prediction models based on 2 combined parameters.

The heat map depicts the color-coded r^2 of each prediction model shown on the left for each contractile parameter shown below at 30 and 120 minutes of reperfusion and for pressure-contractility-matching. N=8. AUC indicates area under the curve; dp/dt_{max} , maximal pressure increase; dp/dt_{min} , maximal pressure decrease; ESP, end-systolic pressure; LDP, laser Doppler perfusion, PCM, pressure-contractility-matching; PP, perfusion pressure; and SecLast, second-last.

normothermic blood perfusion, the monitoring of microvascular circulation relies on higher variation due to the donor heart maintenance in a beating state. This variation can be balanced by calculating the mean

over a more extended period, such as 30 minutes, in the interval-based expression. On the other hand, calculating the mean over long periods can also overshadow small but possibly relevant microvascular flow

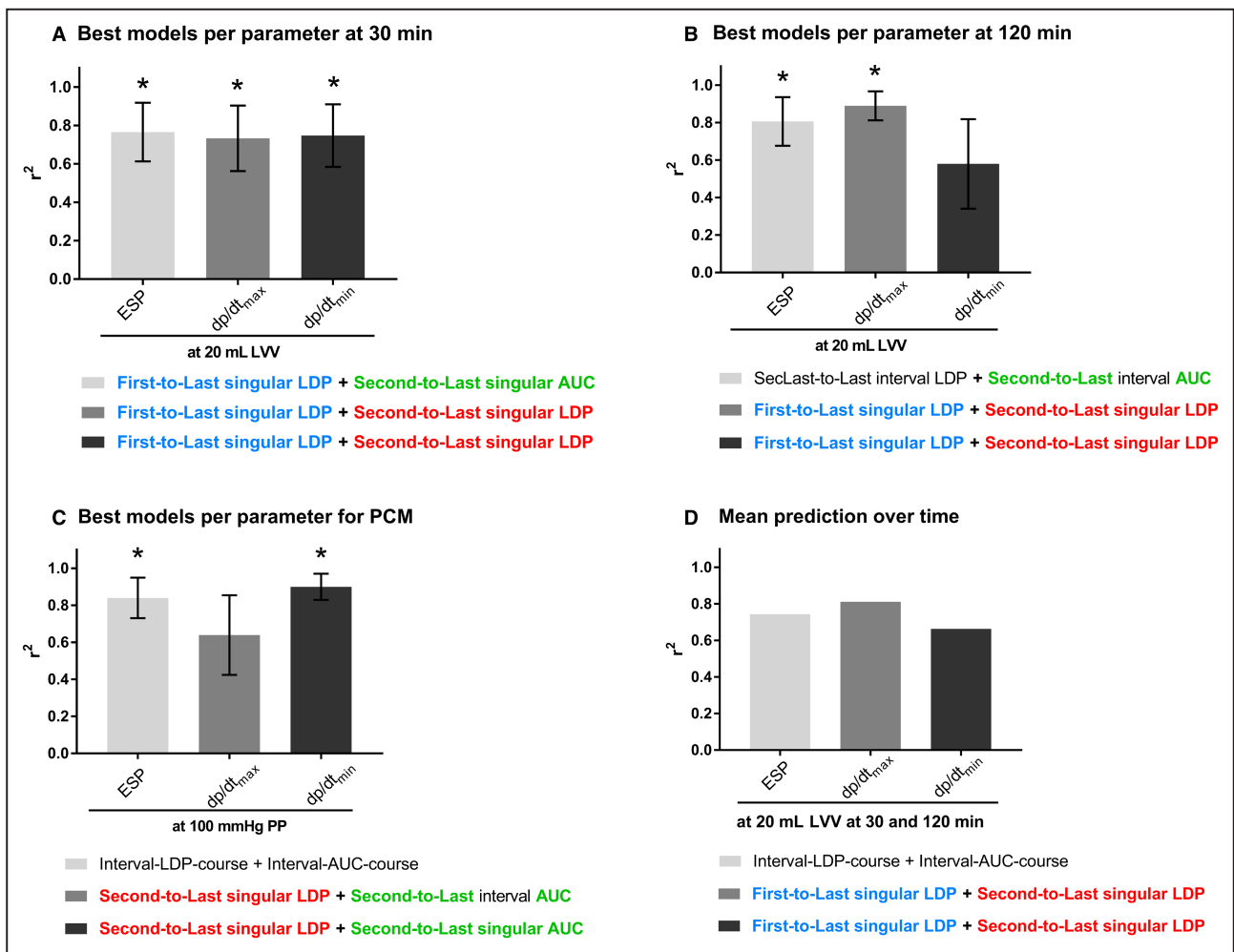


Figure 7. Best prediction models per parameter.

Mean prediction over time was calculated, by calculating the mean of r^2 at 30 and 120 minutes of reperfusion at 20 mL left ventricular volume. Thus, no error bars or significances could be calculated. N=8. AUC indicates area under the curve; dp/dt_{max}, maximal pressure increase; dp/dt_{min}, maximal pressure decrease; ESP, end-systolic pressure; LDP, laser Doppler perfusion; LVV, left ventricular volume; PCM, pressure-contraction matching; PP, perfusion pressure; and SecLast, second-last. * $P < 0.05$.

characteristics. This disadvantage is excluded by calculating “singular” measurements. Additionally, continuous cardioplegic perfusion creates maintenance in a resting state, decreasing perfusion variations.

The model, which predicted most of the contractile parameters best, consists of 2 variables, which reflect microvascular flow shifts between 30 and 60 minutes, so early time points during MP, and the end of the perfusion. From this, we conclude that either the initial period of MP is crucial for contractile performance during reperfusion or the microvascular flow shifts before the end of MP are either less relevant or nonexistent.

The predictability of the diastolic parameter dp/dt_{min} seems to decrease with perfusion time. Obviously, this finding does not indicate a decreased diastolic performance but only a reduced predictability. A possible explanation for this phenomenon could be that diastolic

performance, particularly relaxation of the contracted myocardium, depends more on reperfusion characteristics than on preservation characteristics.^{12,13}

Both LDP and AUC course parameters incorporate not only the microvascular flow shift between only 2 but of multiple time points or periods. Consequently, it is reasonable that the combination of both provide significant predictive information for contractility. Nevertheless, more experiments are needed to verify the present results further. We also want to emphasize that the developed prediction models might be adjusted if more subjects are included. It is also possible that 1 distinct model will be identified to predict every contractile parameter, including perfusion pressure variation.

Microvascular flow shifts occur during hypothermic, crystalloid, cardioplegic MP. We suggest 2 potential

reasons that might explain why microvascular flow shifts predict the contractility and relaxative function of DCD hearts: (1) Even under hypothermic conditions, the metabolism of the heart is only minimized but not eliminated.¹⁴ Therefore, a reduced energy demand still needs to be met and presumably is met by the oxygen, which is diluted in the crystalloid Custodiol-N solution. Consequently, depending on the demands of the individual heart, the microvascular flow is adapted in an autoregulative manner, even under hypothermic conditions. The individual demands, in turn, might depend on the individual characteristics of the donor before and during the induction of circulatory death. (2) Alternatively, a drastically decreased microvascular flow during hypothermic MP potentially is based on microvascular dysfunction that could remain during reperfusion with blood. Microvascular dysfunction, in turn, reduces the myocardial supply, leads to a supply and demand mismatch of cardiomyocytes, and increases the risk of diastolic dysfunction attributable to diastolic cross-bridge cycling.^{15,16} This could also explain the high predictivity of the models for the diastolic parameter dp/dt_{min} . The development of microvascular dysfunction could also depend on donor characteristics. Besides monitoring microvascular flow shifts, the measurement of metabolites could be of great interest in evaluating perfusion quality and myocardial tissue status. Martin et al. showed that succinate accumulation during preservation drives ischemia/reperfusion injury in donor hearts.¹⁴

Monitoring of microvascular flow by LDP technology is feasible and uncomplicated to establish. Using our developed equations, calculation, and quantification of microvascular flow shifts are also possible.⁹ Translating these findings into clinical practice is of high importance for heart transplantation after DCD. First, we could show that perfusion of DCD hearts with the novel Custodiol-N solution reconditions contractile function of DCD hearts in the experimental porcine model. This finding is already worth transferring into clinical practice.⁸ Secondly, the major concern of cardioplegic preservation of DCD hearts, which is the impossibility to evaluate the heart before transplantation, could be dispelled by monitoring microvascular flow shifts during continuous cardioplegic perfusion. Besides, even during normothermic blood perfusion, the heart is evaluated based on visual inspection and lactate clearance. Both criteria allow an evaluation with limited objectivity. Thirdly, although hearts transplanted from brain death donors are not evaluated at the end of transportation in case of the most common preservation method, which still is static cold storage, prediction of contractile function could also be interesting for heart transplantation after brain death if hearts are of higher risk to develop contractile dysfunction. Those include predominantly hearts from donors with

extended criteria, such as hypertrophied hearts, hearts from older donors, or hearts with distant procurement and extended transportation times.

In summary, we demonstrated that microvascular flow shifts occur during hypothermic, crystalloid, cardioplegic MP of hearts in a porcine model of DCD. Additionally, we could show that these flow shifts can predict the contractile function of the heart. This revolutionary finding could be the initial step to translate a potentially superior preservation method for DCD hearts, which is hypothermic crystalloid MP, into the clinical practice.

ARTICLE INFORMATION

Received August 1, 2022; accepted September 12, 2022.

Affiliations

Department of Cardiac Surgery, University Hospital Halle (Saale), University of Halle, Halle (Saale), Germany (L.S., G.V., S.K., A.G., A.S., G.S.); Department of Cardiac Surgery, University Hospital Heidelberg, Heidelberg, Germany (L.S., G.V., S.K., M.K., G.S.); and Faculty Medical and Life Sciences, Furtwangen University, Villingen-Schwenningen, Germany (M.K., F.W.).

Acknowledgments

We gratefully acknowledge the expert technical assistance of Patricia Kraft. Custodiol-N preservation solution was kindly provided by Dr. Franz Köhler Chemie GmbH.

Sources of Funding

None.

Disclosures

None.

Supplemental Material

Table S1

REFERENCES

1. Chew HC, Iyer A, Connellan M, Scheuer S, Villanueva J, Gao L, Hicks M, Harkness M, Soto C, Dinale A, et al. Outcomes of donation after circulatory death heart transplantation in Australia. *J Am Coll Cardiol*. 2019;73:1447–1459. doi: 10.1016/j.jacc.2018.12.067
2. Messer S, Cernic S, Page A, Berman M, Kaul P, Colah S, Ali J, Pavlushkov E, Baxter J, Quigley R, et al. A 5-year single-center early experience of heart transplantation from donation after circulatory-determined death donors. *J Heart Lung Transplant*. 2020;39:1463–1475. doi: 10.1016/j.healun.2020.10.001
3. Tchana-Sato V, Ledoux D, Detry O, Hans G, Ancion A, D'Orio V, Massion PB, Amabili P, Bruls S, Lavigne JP, et al. Successful clinical transplantation of hearts donated after circulatory death using normothermic regional perfusion. *J Heart Lung Transplant*. 2019;38:593–598. doi: 10.1016/j.healun.2019.02.015
4. Shudo Y, Benjamin-Addy R, Koyano TK, Hiesinger W, MacArthur JW, Woo YJ. Donors after circulatory death heart trial. *Future Cardiol*. 2021;17:11–17. doi: 10.2217/fca-2020-0070
5. Scheuer SE, Jansz PC, Macdonald PS. Heart transplantation following donation after circulatory death: expanding the donor pool. *J Heart Lung Transplant*. 2021;40:882–889. doi: 10.1016/j.healun.2021.03.011
6. Messer S, Page A, Axell R, Berman M, Hernández-Sánchez J, Colah S, Parizkova B, Valchanov K, Dunning J, Pavlushkov E, et al. Outcome after heart transplantation from donation after circulatory-determined death donors. *J Heart Lung Transplant*. 2017;36:1311–1318. doi: 10.1016/j.healun.2017.10.021
7. Messer SJ, Axell RG, Colah S, White PA, Ryan M, Page AA, Parizkova B, Valchanov K, White CW, Freed DH, et al. Functional assessment and

- transplantation of the donor heart after circulatory death. *J Heart Lung Transplant*. 2016;35:1443–1452. doi: [10.1016/j.healun.2016.07.004](https://doi.org/10.1016/j.healun.2016.07.004)
8. Saemann L, Korkmaz-Icöz S, Hoorn F, Veres G, Kraft P, Georgevici A-I, Brune M, Guo Y, Loganathan S, Wenzel F, et al. Reconditioning of circulatory death hearts by ex-vivo machine perfusion with a novel HTK-N preservation solution. *J Heart Lung Transplant*. 2021;40:1135–1144. doi: [10.1016/j.healun.2021.07.009](https://doi.org/10.1016/j.healun.2021.07.009)
 9. Saemann L, Wenzel F, Kohl M, Korkmaz-Icöz S, Hoorn F, Loganathan S, Guo Y, Ding Q, Zhou P, Veres G, et al. Monitoring of perfusion quality and prediction of donor heart function during ex-vivo machine perfusion by myocardial microcirculation versus surrogate parameters. *J Heart Lung Transplant*. 2021;40:387–391. doi: [10.1016/j.healun.2021.02.013](https://doi.org/10.1016/j.healun.2021.02.013)
 10. Guide for the Care and Use of Laboratory Animals. 6. National Academy Press; 1996
 11. Leahy MJ, De MFF, Nilsson GE, Maniewski R. Principles and practice of the laser-doppler perfusion technique. *Technol Health Care*. 1999;7:143–162. doi: [10.3233/THC-1999-72-306](https://doi.org/10.3233/THC-1999-72-306)
 12. Slater JP, Amirhamzeh MM, Yano OJ, Shah AS, Starr JP, Kaplon RJ, Burfeind W, Pepino P, Michler RE, Rose EA. Discriminating between preservation and reperfusion injury in human cardiac allografts using heart weight and left ventricular mass. *Circulation*. 1995;92:223–227. doi: [10.1161/01.cir.92.9.223](https://doi.org/10.1161/01.cir.92.9.223)
 13. Singh SSA, Dalzell JR, Berry C, Al-Attar N. Primary graft dysfunction after heart transplantation: a thorn amongst the roses. *Heart Fail Rev*. 2019;24:805–820. doi: [10.1007/s10741-019-09794-1](https://doi.org/10.1007/s10741-019-09794-1)
 14. Martin JL, Costa ASH, Gruszczzyk AV, Beach TE, Allen FM, Prag HA, Hinchy EC, Mahbubani K, Hamed M, Tronci L, et al. Succinate accumulation drives ischaemia-reperfusion injury during organ transplantation. *Nat Metab*. 2019;1:966–974. doi: [10.1038/s42255-019-0115-y](https://doi.org/10.1038/s42255-019-0115-y)
 15. Daud A, Xu D, Revelo MP, Shah Z, Drakos SG, Dranow E, Stoddard G, Kfoury AG, Hammond MEH, Nativi-Nicolau J, et al. Microvascular loss and diastolic dysfunction in severe symptomatic cardiac allograft vasculopathy. *Circ Heart Fail*. 2018;11:e004759. doi: [10.1161/CIRCHEARTFAILURE.117.004759](https://doi.org/10.1161/CIRCHEARTFAILURE.117.004759)
 16. Sinha A, Rahman H, Webb A, Shah AM, Perera D. Untangling the pathophysiological link between coronary microvascular dysfunction and heart failure with preserved ejection fraction. *Eur Heart J*. 2021;42:4431–4441. doi: [10.1093/eurheartj/ehab653](https://doi.org/10.1093/eurheartj/ehab653)

Supplemental Material

Table S1 .Equations.

LDP was either expressed by a singular measurement at the end of each sequence of 30 min or over an interval of 30 min. Index numbers represent the timepoint of perfusion in minutes. a) Applied versions show, which sequences were applied according to our study protocol. b) Generalized versions. AUC: Area under curve. A-Lac, V-Lac, AV-Lac: Arterial, venous or arterio-venous difference of lactate concentration at the end of perfusion. LDP: Laser Doppler Perfusion. rLDP: Relative Laser Doppler Perfusion. PE: End of perfusion.

Formulas to calculate microcirculatory shifts		
SecLast-to-Last singular LDP shift	a)	$\frac{LDP_{240}}{LDP_{210}}$
	b)	$\frac{LDP_{PE}}{LDP_{PE-30 \text{ min}}}$
First-to-Last singular LDP shift	a)	$\frac{LDP_{240}}{LDP_{30}}$
	b)	$\frac{LDP_{PE}}{LDP_{30 \text{ min}}}$
Second-to-Last singular LDP shift	a)	$\frac{LDP_{240}}{LDP_{60}}$
	b)	$\frac{LDP_{PE}}{LDP_{60 \text{ min}}}$
SecLast-to-Last interval LDP shift	a)	$\frac{LDP_{210 \text{ to } 240}}{LDP_{180 \text{ to } 210}}$
	b)	$\frac{LDP_{(PE-30 \text{ min}) \text{ to } PE}}{LDP_{(PE-60 \text{ min}) \text{ to } (PE-30 \text{ min})}}$
First-to-Last interval LDP shift	a)	$\frac{LDP_{210 \text{ to } 240}}{LDP_{0 \text{ to } 30}}$
	b)	$\frac{LDP_{(PE-30 \text{ min}) \text{ to } PE}}{LDP_{0 \text{ to } 30 \text{ min}}}$
Second-to-Last interval LDP shift	a)	$\frac{LDP_{210 \text{ to } 240}}{LDP_{30 \text{ to } 60}}$
	b)	$\frac{LDP_{(PE-30 \text{ min}) \text{ to } PE}}{LDP_{30 \text{ to } 60 \text{ min}}}$
SecLast-to-Last singular AUC shift	a)	$\frac{AUC_{240}}{AUC_{210}}$
	b)	$\frac{AUC_{PE}}{AUC_{PE-30 \text{ min}}}$

First-to-Last singular AUC shift	a)	$\frac{AUC_{240}}{AUC_{30}}$
	b)	$\frac{AUC_{PE}}{AUC_{30 \text{ min}}}$
Second-to-Last singular AUC shift	a)	$\frac{AUC_{240}}{AUC_{60}}$
	b)	$\frac{AUC_{PE}}{AUC_{60 \text{ min}}}$
SecLast-to-Last interval AUC shift	a)	$\frac{AUC_{210 \text{ to } 240}}{AUC_{180 \text{ to } 210}}$
	b)	$\frac{AUC_{(PE-30 \text{ min}) \text{ to } PE}}{AUC_{(PE-60 \text{ min}) \text{ to } (PE-30 \text{ min})}}$
First-to-Last interval AUC shift	a)	$\frac{AUC_{210 \text{ to } 240}}{AUC_{0 \text{ to } 30}}$
	b)	$\frac{AUC_{(PE-30 \text{ min}) \text{ to } PE}}{AUC_{0 \text{ to } 30 \text{ min}}}$
Second-to-Last interval AUC shift	a)	$\frac{AUC_{210 \text{ to } 240}}{AUC_{30 \text{ to } 60}}$
	b)	$\frac{AUC_{(PE-30 \text{ min}) \text{ to } PE}}{AUC_{30 \text{ to } 60 \text{ min}}}$
Interval-rLDP course	a)	$\left(\frac{LDP_{30 \text{ to } 60}}{LDP_{0 \text{ to } 30}} + \frac{LDP_{60 \text{ to } 90}}{LDP_{30 \text{ to } 60}} + \frac{LDP_{90 \text{ to } 120}}{LDP_{60 \text{ to } 90}} + \frac{LDP_{120 \text{ to } 150}}{LDP_{90 \text{ to } 120}} + \frac{LDP_{150 \text{ to } 180}}{LDP_{120 \text{ to } 150}} + \frac{LDP_{180 \text{ to } 210}}{LDP_{150 \text{ to } 180}} + \frac{LDP_{210 \text{ to } 240}}{LDP_{180 \text{ to } 210}} \right) / 7$
	b)	$\left(\frac{LDP_{30 \text{ to } 60 \text{ min}}}{LDP_{0 \text{ to } 30 \text{ min}}} + \frac{LDP_{60 \text{ to } 90 \text{ min}}}{LDP_{30 \text{ to } 60 \text{ min}}} + \dots + \frac{LDP_{(PE-30 \text{ min}) \text{ to } PE}}{LDP_{(PE-60 \text{ min}) \text{ to } (PE-30 \text{ min})}} \right) /$ $(N_{\text{sequences of } 30 \text{ min}} - 1)$
Interval-rAUC course	a)	$\left(\frac{AUC_{30 \text{ to } 60}}{AUC_{0 \text{ to } 30}} + \frac{AUC_{60 \text{ to } 90}}{AUC_{30 \text{ to } 60}} + \frac{AUC_{90 \text{ to } 120}}{AUC_{60 \text{ to } 90}} + \frac{AUC_{120 \text{ to } 150}}{AUC_{90 \text{ to } 120}} + \frac{AUC_{150 \text{ to } 180}}{AUC_{120 \text{ to } 150}} + \frac{AUC_{180 \text{ to } 210}}{AUC_{150 \text{ to } 180}} + \frac{AUC_{210 \text{ to } 240}}{AUC_{180 \text{ to } 210}} \right) / 7$
	b)	$\left(\frac{AUC_{30 \text{ to } 60 \text{ min}}}{AUC_{0 \text{ to } 30 \text{ min}}} + \frac{AUC_{60 \text{ to } 90 \text{ min}}}{AUC_{30 \text{ to } 60 \text{ min}}} + \dots + \frac{AUC_{(PE-30 \text{ min}) \text{ to } PE}}{AUC_{(PE-60 \text{ min}) \text{ to } (PE-30 \text{ min})}} \right) /$ $(N_{\text{sequences of } 30 \text{ min}} - 1)$